



HAL
open science

Altering the Bio-inert Properties of Surfaces by Fluorinated Copolymers of mPEGMA

Ryohei Koguchi, Katja Jankova, Yukiko Tanaka, Aki Yamamoto, Daiki Murakami, Qizhi Yang, Bruno Ameduri, Masaru Tanaka

► **To cite this version:**

Ryohei Koguchi, Katja Jankova, Yukiko Tanaka, Aki Yamamoto, Daiki Murakami, et al.. Altering the Bio-inert Properties of Surfaces by Fluorinated Copolymers of mPEGMA. *Biomaterials Advances*, 2023, 153, pp.213573. 10.1016/j.bioadv.2023.213573 . hal-04179017

HAL Id: hal-04179017

<https://hal.science/hal-04179017v1>

Submitted on 8 Aug 2023

HAL is a multi-disciplinary open access archive for the deposit and dissemination of scientific research documents, whether they are published or not. The documents may come from teaching and research institutions in France or abroad, or from public or private research centers.

L'archive ouverte pluridisciplinaire **HAL**, est destinée au dépôt et à la diffusion de documents scientifiques de niveau recherche, publiés ou non, émanant des établissements d'enseignement et de recherche français ou étrangers, des laboratoires publics ou privés.

Altering the Bio-inert Properties of Surfaces by Fluorinated Copolymers of *m*PEGMA

Ryohei Koguchi,¹ Katja Jankova,^{2,3} Yukiko Tanaka,² Aki Yamamoto,² Daiki Murakami,²

*Qizhi Yang,⁴ Bruno Ameduri,^{4**} Masaru Tanaka^{2**}*

¹ AGC Inc. Organic Materials Division, Materials Integration Laboratories, 1-1 Suehiro-cho, Tsurumi-ku, Yokohama, Kanagawa 230-0045, Japan

² Soft Materials Chemistry, Institute for Materials Chemistry and Engineering, Kyushu University, Build. CE41, 744 Motooka Nishi-ku, Fukuoka, 819-0395, Japan

³ Department of Energy Conversion and Storage, Technical University of Denmark, Elektrovej, Build. 375, 2800 Kongens Lyngby, Denmark

⁴ University of Montpellier, ICGM, CNRS, ENSCM, 34000 Montpellier, France

Abstract

Hydrophilic materials display “bio-inert properties,” meaning that they are less recognized as foreign substances by proteins and cells. Such materials are often water soluble; therefore, one

general approach to enable the use of these materials in various applications is by copolymerizing hydrophilic monomers with hydrophobic ones to make the copolymers water insoluble. However, reducing the amount of hydrophilic monomers may reduce the bio-inert properties of the material. The decrease in bio-inert properties can be avoided when small amounts of fluorine are used in copolymers with hydrophilic monomers, as presented in this article. Even in small quantities (7.9 wt%), the fluorinated monomer 1,1,1,3,3,3-hexafluoropropan-2-yl 2-fluoroacrylate (FAHFiP) contributed to the improved hydrophobicity of the polymers of the long side-chain poly(ethylene glycol) methyl ether methacrylate (*m*PEGMA) bearing nine ethylene glycol units turning them water insoluble. As evidenced by the AFM deformation image, a phase separation between the FAHFiP and *m*PEGMA domains was observed. The copolymer with the highest amount of the fluorinated monomer (66.2 wt%) displayed also high (82%) FAHFiP amount at the polymer–water interface. In contrast, the hydrated sample with the lowest FAHFiP/highest *m*PEGMA amount was enriched of three times more hydrophilic domains at the polymer–water interface compared to that of the sample with the highest FAHFiP content. Thus, by adding a small FAHFiP amount to *m*PEGMA copolymers, water insoluble in the bulk too, could be turned highly hydrophilic at the water interface. The high content of intermediate water contributed to their excellent bio-inert properties. Platelet adhesion and fibrinogen adsorption on their surfaces were even more decreased as compared to those on poly(2-methoxyethyl acrylate), which is typically used in medical devices.

KEYWORDS

Bio-inert properties; Fluorinated copolymers; Hydration structure; Intermediate water; *m*PEGMA

1. Introduction

To avoid inflammation and other injury processes, any material, including those of medical devices that come in contact with blood, needs to be blood compatible or bio-inert, which means resistant to adhesion of biomolecules such as blood, cells, and proteins.^{1,2} In general, hydrophilic materials exhibit such properties because they contain intermediate water (*IW*), that is, water molecules that are loosely bound to a polymer. To date, poly(2-methoxyethyl acrylate) (PMEA) is the known water-insoluble homopolymer that contains *IW* in the hydrated state and exhibits excellent blood compatibility.³ Thin films on numerous materials and medical devices can be straightforwardly cast from methanol solutions of PMEA,⁴⁻⁶ thereby preventing contact between blood and the substrate.

Distinctive bio-inert polymers include poly(ethylene glycol) (PEG),⁷ polyethylene glycol (methylether)methacrylates (*m*PEGMA),⁸ and zwitterionic polymers,⁹ which are all water soluble. Their solubility in water limits their direct use in applications that require strategies conducted under conditions preserving their bio-inert characteristics.² Modulating the biocompatibility of polymer surfaces was historically achieved by several approaches: suitable modification of functional polymers, surfaces or particles, followed by coupling (or lately “clicking”) with hydrophilic polymers;¹⁰⁻¹³ surface-initiated polymerizations of hydrophilic monomers employing various techniques;¹⁴⁻²⁰ and copolymerization with a hydrophobic monomer using either conventional, controlled radical (RDRP) or other polymerization techniques to yield various architectures.²¹⁻²⁸ We recently reviewed these strategies and identified the requirements for designing bio-inert materials.²

PEGylation or general hydrophilization of surfaces has been realized using PEG, *m*PEGMA, PMEA, or other hydrophilic polymers. Due to the anti-PEG immune response still limiting the efficacy of PEGylated treatments although there were many clinical trials, other non – ethylene oxide (EO) containing polymers are searched.²⁹ However, copolymers with EO units are ideal models for studying the mechanisms of blood compatibility. Hence, exploring this possibility is of considerable interest.

On the other hand, hydrophobic materials such as fluorinated polymers are chemically inert, durable, and oil and water repellent owing to their ultra-low surface energy.³⁰⁻³⁷ These properties impart stability in the human body. Therefore, fluoropolymers are also applied in many medical devices. However, these polymers do not usually contain any hydrophilic groups and are bio-inert only for a limited time. Therefore, fluorinated materials should be further improved. One possibility deals with copolymerizing a fluorinated monomer with a hydrophilic one that may induce a phase separation enabling hydration structure changes.³⁸ Owing to the easy phase separation of fluorinated groups, various fluorinated copolymers based on hydrophilic monomers have been synthesized, and their bio-inert characteristics have been investigated.^{2,39,40} Actually, several ternary block copolymers with hydrophilic and both non-halogenated and fluorinated hydrophobic groups exhibited minimal protein adsorption at a constant rate,³⁹ and were more hydrophilic than those containing no fluoromonomer when in contact with water.⁴¹ Indeed, -CF₃ groups segregate at the polymer–air interface and are supposed to flip in water because they exhibit less cohesive energy than -CH₃, thus exposing the hydrophilic part to water and making the surface less hydrophobic. Random copolymers based on 2-hydroxyethyl methacrylate (HEMA) and several molar percent of 2-perfluorooctylethyl methacrylate (FMA)⁴² have shown minimum adsorption of bovine serum albumin or the human plasma fibrinogen (HFG) in

compositions where FMA was copolymerized with 7.56 and 2.45 mol.% HEMA, respectively. However, to the best of our knowledge, the blood compatibility / bio-inertness of fluorinated PEG copolymers has never been investigated, influenced by only the fluorine block.

We have recently summarized by various examples² that fluorinated sequences, initiators, or monomers in small quantities with hydrophilic monomers form copolymers which efficiently phase-separate. Indeed, in the presence of water, the surface becomes more hydrophilic and displays bio-inert properties.^{2,39,40}

The relationship between the physical and bio-inert properties of materials depends on the surface charge and microstructure, critical surface tension, and glass transition temperature. Given the change that the interface undergoes when water approaches, the hydration state of the organic and inorganic materials should be determined. This assessment can be quantitatively performed using differential scanning calorimetry (DSC). In addition to hydrophilicity, the presence of water, particularly *IW*, is an important parameter for bio-inert material interfaces. We found *IW* using DSC in numerous materials that turned out to be blood compatible.⁴³⁻⁴⁷ Although *IW* is crucial, its behavior needs to be understood by discussing DSC data of any investigated material in relation with the hydration state of the interface, as quantified by contact angle (CA), atomic force microscopy (AFM), and X-ray photoelectron spectroscopy (XPS). Moreover, water molecules in the polymer matrix have also been observed by solid-state ¹H NMR to change their mobility through molecular interactions with the polymer chains. Such a tendency has been observed in copolymers based on HEMA and small amounts of either 2-(dimethylamino)ethyl methacrylate (DMAEMA)⁴⁰ or 2,2,2-trifluoroethyl methacrylate (TFEMA).^{39,40} While the facts found so far^{2,39,40} are important for understanding the mechanism of biocompatibility that relies

on the *IW* concept, improving hydrophobicity is one of the major advantages when considering industrial applications.

To ensure high mobility of the polymer chains in hydrated state, the dry T_g of the hydrophilic part has to be as low as possible that in principal decreases in the hydrated state. *m*PEGMA is a water-soluble polymer with a T_g in the dry state lower than that of both *m*PEG and PMEA. *m*PEGMA, which contained nine EO units in the side chain, was therefore an ideal hydrophilic polymer that could contribute to the improvement of bio-inert properties when polymerized with a small amount of a fluorine monomer.

Here, following investigations dealing with small amounts of fluorinated monomers in copolymers with hydrophilic polymers,^{2,39,40} we designed and synthesized new fluorinated copolymers based on the alpha-fluoroacrylate monomer, 1,1,1,3,3,3-hexafluoropropan-2-yl 2-fluoroacrylate (FAHFiP).⁴⁸ FAHFiP can be radically polymerized and has a high fluorine content; therefore, a small amount of FAHFiP in copolymers with *m*PEGMA is expected to make the copolymers insoluble in water. An optimal composition for the development of bio-inert properties has been reported for fluorinated moieties and PEG block polymers. However, many achievements were only discussed based on the information at the air interface.^{49,50} In this work, the hydration structures of the synthesized water-insoluble copolymers of different compositions were examined by comparing the air with the polymer–water interface. Furthermore, platelet adhesion, protein adsorption, and the relationship between the hydration structure and bio-inert properties, were comprehensively evaluated.

2. Experimental

2.1. Materials

1,1,1,3,3,3-Hexafluoropropan-2-yl 2-fluoroacrylate (FAHFiP) was purchased from Scientific Industrial Application P and M, Russia and used as received. Poly(ethylene glycol) methyl ether methacrylate (*m*PEGMA) was purchased from Sigma-Aldrich (average M_n 500, containing 100 ppm MEHQ and 200 ppm BHT as inhibitors) and used after purification by passing through a short column of basic aluminum oxide. *tert*-Butyl peroxyvalate (TBPPi) was kindly supplied by Akzo Nobel (purity 75%, Compiègne, France).

2.2. Syntheses of copolymers

The typical experimental procedure for Sample 2 is presented as follows:

FAHFiP (2413.3 mg, 10.05 mmol, 49.16 eq.), *m*PEGMA (5040.0 mg, 10.08 mmol, 41.2 eq.) and TBPPi (95.0 mg, 0.4089 mmol, 2.0 eq.) were added to a 100 mL round bottom flask, and 28.0 g acetonitrile was used as the solvent. The solution was deoxygenated by nitrogen bubbling for 40 min, and then polymerization was initiated by placing the flask in an oil bath at 65 °C. After 2.5 h, copolymerization was stopped by exposure to air. The copolymer was purified twice by evaporating the solvent under reduced pressure and precipitated from pentane as a transparent viscous solid. ^{19}F and ^1H NMR spectroscopies (Figures S1, S2 and S3) enabled to assess the monomer conversions and the results are displayed in Table 1.

Table 1. Feed molar ratios and monomer conversions (assigned by ^{19}F and ^1H NMR spectroscopy) from the conventional radical copolymerizations of FAHFiP with *m*PEGMA (in 28 g acetonitrile as the solvent)

Copolymers	Feeding ratio (mol %) [FAHFiP] ₀ /[<i>m</i> PEGMA] ₀ /[TBPPi] ₀	Conversion (%)	
		FAHFiP	<i>m</i> PEGMA

Sample 1	80:20:2	99.7	~100
Sample 2	55:45:2	91.9	~100
Sample 3	20:80:3	~100	93.7

2.3. Analyses.

2.3.1) Characterization of the chemical structure of the obtained polymers

The poly(FAHFiP-*co*-mPEGMA) copolymers were characterized using ^1H and ^{19}F NMR spectroscopy. The spectra were recorded on a Bruker AC 400 spectrometer (400 MHz for ^1H and 376 MHz for ^{19}F) using acetone- d_6 as the solvent. The coupling constants and chemical shifts are given in hertz (Hz) and parts per million (ppm), respectively. The instrumental parameters for recording ^1H [or ^{19}F] NMR spectra were as follows: flip angle 90° [or 30°], acquisition time 4.5 s [or 0.7 s], pulse delay 2 s [or 5 s], number of scans 32 [or 64], and a pulse width of 5 μs for ^{19}F NMR.

Molar masses were determined by gel permeation chromatography (GPC) using the integrated size-exclusion chromatogram (SEC) unit of a Tosoh HLC-8320 chromatograph equipped with three Styragel HR columns connected in series (WAT044229, WAT044241, and WAT044235) and a refractive index detector. Measurements were performed with dimethylformamide (DMF) as an eluent, containing 10 mM lithium bromide, at 40°C with a 1.0 mL/min flow. Molar masses were calculated using PEG standards with narrow dispersity in the range of 1.96×10^3 – 1.02×10^6 g/mol.

2.3.2) Thermal property evaluation and quantification of interactions between water and (co)polymers.

DSC measurements were performed using a Q1000 from TA Instruments and X-DSC7000 (Seiko Instruments, Japan) in the temperature range of -100 to 150 °C at a heating rate of 5 °C min^{-1} under nitrogen. Dry and hydrated T_g temperatures were determined automatically by the instrument from the second heating trace and reported as the midpoint of the thermal transition. The hydrated sample was prepared and the amount of hydration water in the hydrated polymers was analyzed using a previously reported method.^{43,44,46} The hydrated samples were prepared by immersion in ultrapure water for more than 3 days before measurement.

Normally, the amounts of different types of water in water-insoluble polymers are discussed at the equilibrium water content (EWC) of the polymers estimated by DSC as the water content at which a peak for the melting of ice at approximately 0 °C (free water) and a small shoulder or peak for melting of *IW* appear below the temperature. In the present study, however, the amount of *IW* at the EWC cannot be determined because of the presence and crystallization of free water resulting in unclear exothermic peak of the *IW*. Therefore, we determined the *IW* amount in each polymer at a water content immediately below the EWC. The water content is given by Equation (1):

$$\text{WC (wt\%)} = ((W_1 - W_0) / W_1) \times 100, \quad (1)$$

where W_0 and W_1 stand for the weights of the dry and hydrated samples, respectively.

The amounts of different types of water in the hydrated polymers are given by the following equation:

$$\text{WC (wt\%)} = \text{NFW (wt\%)} + \text{IW (wt\%)} + \text{FW (wt\%)} \quad (2)$$

$$\text{IW (wt\%)} = \Delta H_{cc} / 334 (\text{Jg}^{-1}) \quad (3)$$

$$\text{FW (wt\%)} = (\Delta H_m / 334(\text{Jg}^{-1})) - \text{IW} \quad (4)$$

ΔH_{cc} and ΔH_m are enthalpy changes during the cold crystallization and melting of ice, respectively.

2.3.3) Preparation and characterization of the polymer surfaces^{43,44,46}

Film samples, which were used for CA and XPS measurements and characterized by AFM and human blood platelet adhesion test, were prepared as follows: Polymer samples were dissolved in acetonitrile or methanol (0.2 wt /vol % solution) and filtered. The solution was spin-coated onto round-shaped 14 mm ϕ substrates and washed with methanol prior to coating the surface. The substrates were coated twice with the solution using a Mikasa spin coater MS-A100 at rates of 500 rpm for 5 s, 2000 rpm for 10 s, slope for 5 s, 4000 rpm for 5 s, and slope for 4 s. Subsequently, the substrates were dried at room temperature for 24 h.

The water CAs (WCAs) on the polymer-coated surface were measured at 25 °C using the sessile drop method. Captive bubble method was used to evaluate hydrated surfaces. In this method, 2 μ L of air bubbles were injected beneath the hydrated surface immersed in water. The reported values for both measurements were the average of three measurements made at different positions on the substrate.

XPS measurements were performed on an ESCA-5500 (Physical Electronics, Inc.) equipped with a monochromatic Al $K\alpha$ X-ray source. The measurements were conducted at a photoelectron takeoff angle (measured with respect to the plane of the sample) of 45° relative to the polymer-coated substrates. Charge compensation was achieved by using a low-energy electron flood gun.

The interfacial features of the samples were observed in water using AFM (Bioscope Resolve, Bruker, Billerica, MA, USA) with cantilever ScanAsyst-fluid (spring constant $k = 0.35$

N/m, tip radius < 12 nm; Bruker). The features were observed in the peak force tapping mode at 37 °C, at 1 and 24 h after immersion in water. Data analyses were performed using a NanoScope Analysis 1.8 (Bruker).

2.3.4) Preparation and characterization of the polymer surfaces

Micro bicinchoninic acid (BCA) assay was performed to measure the amount of adsorbed proteins on the polymer surfaces. Fibrinogen (Sigma) was used as the protein, and the analyses were performed as previously reported.^{43,44,46} The polymer surfaces were prepared for micro BCA assay in the following manner: 15 µL of the polymer solution (0.2 wt/vol %) in ethanol was added to a polypropylene 96-well plate. The plate was slowly air-dried for 3 days at room temperature. Then, 50 µL of 1 mg/mL fibrinogen in phosphate-buffered saline (PBS) were added to each well and incubated for 10 min at 37 °C. The wells were then washed for five times with 200 µL PBS. The adsorbed proteins were extracted using a solution of 5% sodium dodecyl sulfate and 0.1 N NaOH via incubation for 10 min at 37 °C. The extracted proteins were assessed using the micro-BCA assay (Thermo Scientific, Rockford, IL, USA) according to the manufacturer's instructions. The amount of protein was calculated using the albumin standard curve.

2.3.5) Preparation of Polymer Substrates and Human Platelet Adhesion Test

The polymer substrates used in human platelet adhesion tests were prepared as follows: polymer-coated substrates were cut into 8 mm × 8 mm squares and then affixed to a scanning electron microscope (SEM) specimen stage using double-sided tape. Platelet-rich plasma and platelet-poor plasma were obtained from human blood by two stages of centrifugation at 400

relative centrifugal force (rcf) for 5 minutes and 2500 rcf for 10 minutes, respectively.^{43,44,46}

SEM was used to quantify the number of platelets adhering to the substrates. For statistical purposes, the platelet adhesion test was performed once using human blood. The reported values were the averages of five measured points on three different films.

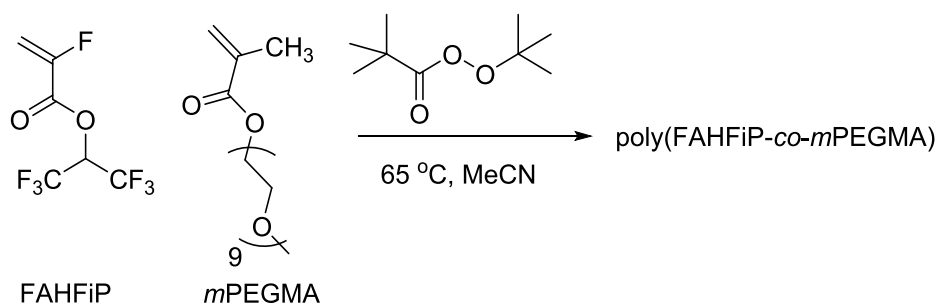
2.3.6) Statistical analysis

All data were expressed as mean \pm standard deviation (SD). *P* is an abbreviation for *P* value that is the probability to obtain test results at least as extreme as the result actually observed under the assumption that the null hypothesis is correct. Differences with *P* values of less than 0.05 were considered statistically significant.

3. Results and discussion

3.1. Syntheses and characterization of the poly(FAHFiP-*co*-*m*PEGMA) copolymers

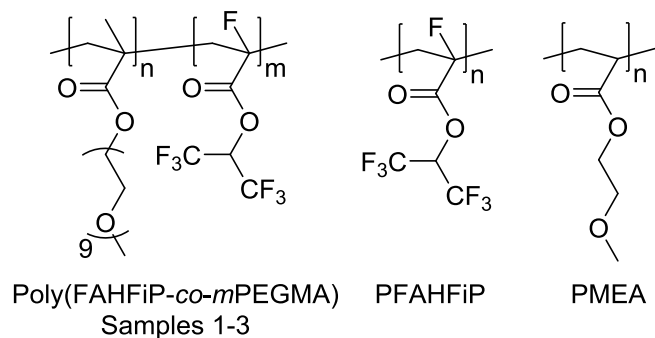
Poly(FAHFiP-*co*-*m*PEGMA) copolymers were synthesized by conventional radical copolymerizations of FAHFiP with *m*PEGMA initiated by *tert*-butyl peroxyvalate (TBPPi) in acetonitrile at 65 °C (Scheme 1).



Scheme 1. Synthesis route to poly(FAHFiP-*co*-*m*PEGMA) copolymers, FAHFIP and *m*PEGMA standing for 1,1,1,3,3,3-hexafluoropropan-2-yl 2-fluoroacrylate and poly(ethylene glycol) methyl ether methacrylate, respectively.

The kinetics of α -fluoroacrylates with alkyl methacrylates have already been reported by several authors. First, Pittman et al.⁵¹ carried out the copolymerization α - fluoroacrylates with MMA and determined their corresponding reactivity ratios: $r_{\alpha\text{-F-acrylate}} = 0.36$, $r_{\text{MMA}} = 1.17$ at 50 °C. Then, Cracowski et al.⁵² studied the kinetic of radical copolymerization of 2,2,2- trichloroethyl α - fluoroacrylate (FATRICE) with 2,2,2- trifluoroethyl methacrylate (MATRIFE) and assessed their reactivity ratios ($r_{\text{MATRIFE}} = 1.52$ and $r_{\text{FATRICE}} = 0.61$ at 74 °C). A third investigation also determined the kinetic constants for the copolymerization of 2,2,2-trifluoroethyl α - fluoroacrylate (FATRIFE) with 2-trifluoromethacrylic acid (MAF) as follows: $r_{\text{FATRIFE}} = 1.65 \pm 0.07$ and $r_{\text{MAF}} = 0$ at 56 °C According to these studies, the resulting copolymers based on α -fluoroacrylates were statistic.⁴⁸

After reaction, these copolymers were purified by precipitation from pentane and dried. In addition, and compared to such copolymers, owing to its hydration structure,³ PMEA was also prepared as a reference polymer for this present study. Because of its bio-inert properties, this homopolymer is known for its medical applications.^{4,6} The structures of all polymers used in the investigation are presented in Scheme 2.



Scheme 2. Chemical structures of the poly(FAHFiP-*co*-*m*PEGMA) copolymers, PFAHFiP, and PMEA.

Given the low refractive indices of fluoropolymers, the SEC signals assigned to the poly(FAHFiP) homopolymer and poly(FAHFiP-*co*-*m*PEGMA) copolymer containing a high FAHFiP content (Figure 1) are negative, as already reported.^{53,54} Additionally, PFAHFiP exhibited shoulders at high retention time, which were also detected in the copolymers. Even after purification and as expected, the three copolymers displayed bi- or tri-modal polydispersities (Figure 1) owing to the imperfection of the conventional radical copolymerization of these comonomers and possible transfer to acetonitrile. NMR and DSC were used to characterize such copolymers under both dry and hydrated conditions (Table 2 and Figure 2).

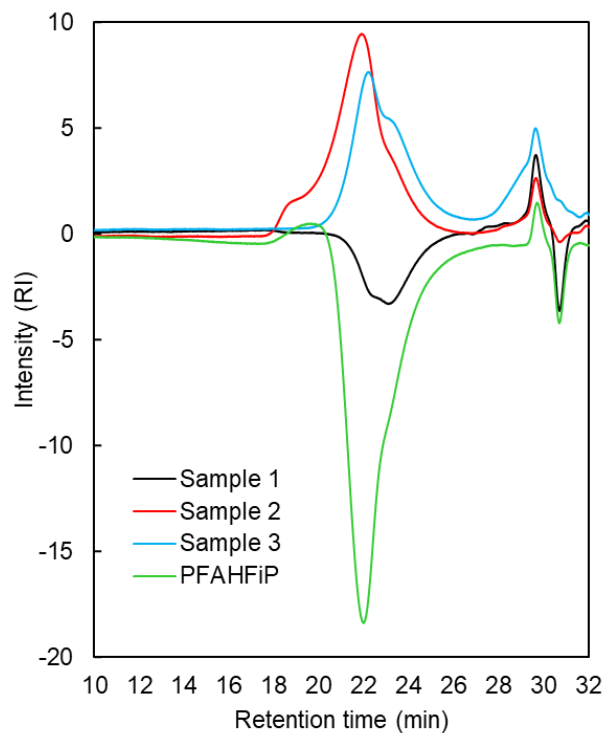


Figure 1. SEC overlays of PFAHFiP and poly(FAHFiP-*co*-*m*PEGMA) copolymers synthesized and used in the present study.

Table 2. Compositions, molar mass characteristics, and glass transition temperatures of the (co)polymers used in the investigation.

Polymers	fluorinated monomer content [*]		T_g °C ^{**}		M_n ^{***} (g/mol)	PDI
	mol %	wt%	dry	hydrated		
Sample 1	80.3	66.2	N.D.****	-74	11600	1.77
Sample 2	45.4	28.5	-50	-72	26600	4.51
Sample 3	15.2	7.9	-58	-71	13500	2.17
PFAHFiP	100	100	103	>50	17100	2.00
PMEA	0	0	-35	-50	22000	2.81

* Calculated by ^1H -NMR spectroscopy

** Calculated from DSC (heating)

*** GPC analysis was carried out in DMF using PEG standards except for that of PMEA, which was carried out in tetrahydrofuran using polystyrene standards.

**** N.D.= not detected

The FAHFiP and *m*PEGMA conversions were determined from the ^{19}F and ^1H NMR spectra of the crude products, respectively, and calculated using Equations 5–7. The FAHFiP conversion was determined using Equation 5: The signals in the pendent group ($-\text{CH}(\text{CF}_3)_2$) were located between -73.90 and -74.12 ppm before polymerization while they shifted to the -74.12 and -74.90 ppm range and became broader after polymerization. The *m*PEGMA conversion was deduced from Equation 6. The signals assigned to the vinyl group from the unreacted monomer were found at 6.09 and 5.64 ppm, whereas that of methylene in $\text{C}(=\text{O})\text{O}-\text{CH}_2\text{CH}_2-$ was centered at 4.26 ppm. However, after polymerization, the signals of unsaturated end group disappeared to yield multiplet between 0.8 and 1.4 ppm while that of methylene shifted into the 3.35-4.32 ppm range. The FAHFiP conversion was also determined by ^1H NMR spectroscopy using Equation 7.

$$\text{Conv}_{(\text{FAHFiP})}(\%) = \frac{\int_{-74.90}^{-74.12} \text{CF}_3 \text{ of polyFAHFiP unit}}{\int_{-74.90}^{-74.12} \text{CF}_3 \text{ of polyFAHFiP unit} + \int_{-74.12}^{-73.90} \text{CF}_3 \text{ of FAHFiP monomer}} \times 100 \quad (5)$$

$$\text{Conv}_{(m\text{PEGMA})}(\%) = 100 - \frac{2 \times \int_{5.67}^{5.62} \text{CH of vinyl group from } m\text{PEGMA}}{\int_{4.32}^{3.35} \text{CH}_2 \text{ of the methylene connected to the ester bond of } m\text{PEGMA}} \times 100 \quad (6)$$

$$\text{Conv}_{(\text{FAHFiP})}(\%) = 100 - \frac{\int_{5.89}^{5.82} \text{CH of vinyl group from FAHFiP}}{\int_{6.63}^{6.15} \text{CH from both FAHFiP monomer and polyFAHFiP unit}} \times 100 \quad (7)$$

As observed from the data in Table 2, from Samples 1 to 3, the fluoromonomer content in the synthesized copolymers decreased, whereas that in *m*PEGMA increased. As expected, both T_g values of the dry and hydrated copolymers (Figure 2) were lower than those of PMEA, which was considered in the design of these copolymers. Surprisingly, Sample 3, which contained 15.2 mol % (7.9 wt%) only of FAHFiP, was water-insoluble. This result shows that a small FAHFiP amount significantly contributes to the hydrophobicity of the copolymers. In contrast, a previous example in which *m*PEGMA was copolymerized with 60.0 mol % (43.2 wt%) of a typical hydrophobic, long-chain hydrocarbon monomer lauryl methacrylate⁵⁵ was water soluble.

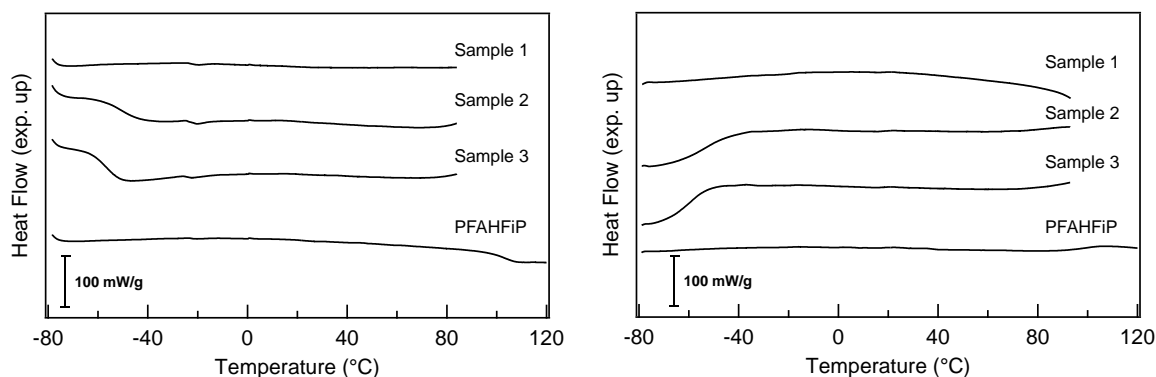


Figure 2. DSC thermograms for evaluation of the T_g of dry samples at heating (left) and cooling (right) conditions.

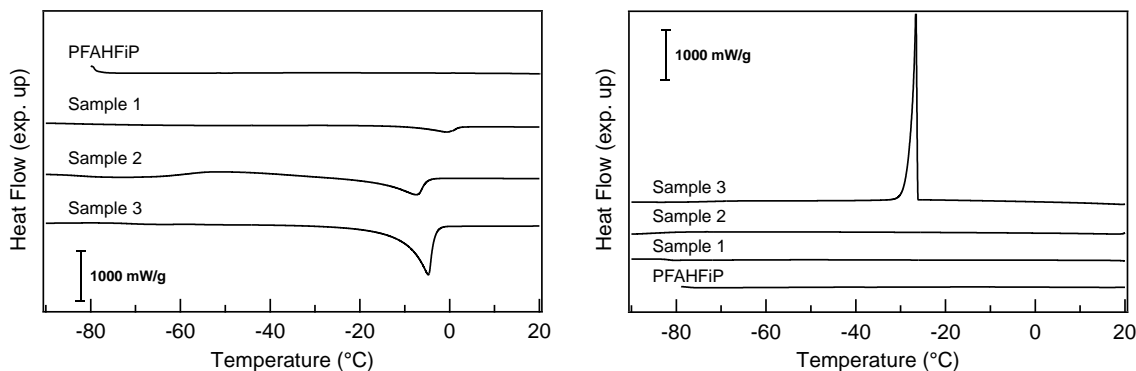


Figure 3. DSC thermograms for the hydrated structures immediately below the EWC at heating (left) and cooling (right) conditions.

3.2. Hydrated structures

The hydrated structures of the polymers are presented in Table 3. Detailed evaluations of poly(FAHFiP-*co*-*m*PEGMA) copolymers and PFAHFiP as well as DSC profiles at different water contents are presented in Figures S4–S7. There is only a small *IW* amount in Sample 1 that has the highest FAHFiP content. When the FAHFiP content in copolymers 1, 2, and 3 decreased, the IWC increased (Figure 3). This increased IWC content is expected to further influence the bio-inert properties of the new copolymers relative to those of PMEA. Table 3 exhibits the DSC data for the hydrated structures in the EWC.

Table 3. Water content in the (co)polymers for the different kinds of water.

	WC	NFW	IW_{heating}	IW_{cooling}	IW_{total}	FW
	(wt%)	(wt%)	(wt%)	(wt%)	(wt%)	(wt%)
Sample 1	19.8	18.1	1.7	0.0	1.7	0.0
Sample 2	31.7	21.6	10.1	0.0	10.1	0.0
Sample 3	54.4	31.2	0.1	22.2	22.3	0.0
PFAHFiP	0.7	0.7	0.0	0.0	0.0	0.0
PMEA*	8.7	2.5	3.7	0.0	3.7	2.5

*Water amounts for PMEA were determined at EWC⁴⁴

3.3. Surface properties of substrates coated with poly(FAHFiP-co-mPEGMA) copolymers

To investigate the surface properties of the materials used, contact angles (CAs) and X-ray photoelectron spectroscopy (XPS) measurements were conducted under dry and hydrated conditions.

3.3.1. Contact angle (CA) measurements

The CAs of the dry and hydrated (co)polymers were determined using both the sessile drop and bubble in water methods to determine the water CA (WCA) and air-in-water CA (ACA), respectively. ACA, which should approximate 180-WCA, is an excellent indicator of hydrophilicity.² The data are presented in Table 4 and Figure 4. As expected, polyethylene terephthalate (PET) and the fluorine containing homopolymers are hydrophobic, the WCA curve of Sample 2 overlapping with that of PET. Sample 1 was similarly hydrophobic (WCA= ~ 100°). Over time, the WCAs of PET, fluorinated homopolymers, and Sample 1 were stable for 60 seconds, whereas those of Samples 2 and 3 decreased. Copolymer Samples 2 and 3 exhibited intermediate hydrophilicity with WCA of 75° and 58°, which corresponded to the ACA of 140°

and 144°, respectively. Water contact angle image of fluorinated copolymers, PMEA and PET after 60 seconds of dropping are presented in Figure S8. However, their WCA and ACA values were considerably higher than those of the PMEA. To understand the situation at the polymer–water interface, XPS and AFM analyses were performed.

Table 4. Contact angle values of poly(FAHFiP-*co*-*m*PEGMA) copolymers, PFAHFiP, and PMEA. The data represent the means \pm SD ($n = 3$).

Polymers	Sessile drop (WCA)		Captive bubble (ACA)
	1 s	60 s	16 h
Sample 1	103.3 \pm 0.7	99.9 \pm 1.3	142.7 \pm 0.9
Sample 2	81.4 \pm 0.5	75.1 \pm 1.1	139.7 \pm 0.3
Sample 3	65.1 \pm 1.6	58.1 \pm 0.6	143.8 \pm 0.7
PFAHFiP	99.3 \pm 2.1	96.9 \pm 1.6	109.4 \pm 1.1
PMEA	68.5 \pm 4.2	38.2 \pm 2.0	130.6 \pm 0.8
PET	81.1 \pm 1.2	76.0 \pm 0.9	109.5 \pm 4.8

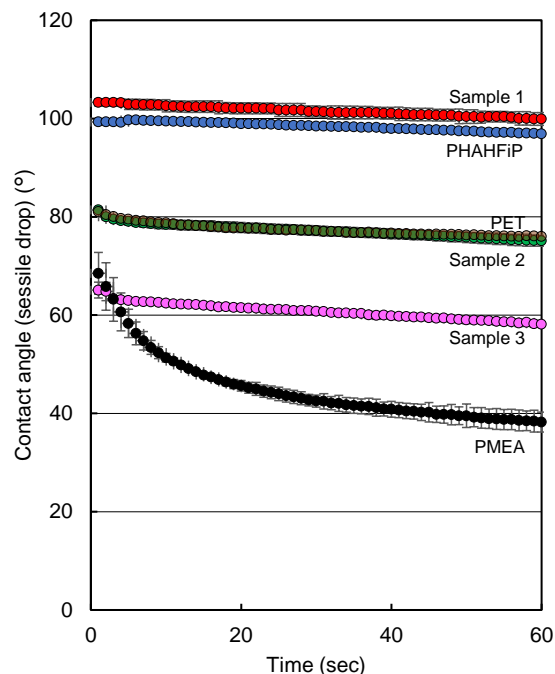


Figure 4. Time dependence of WCA on the surface of all investigated polymers. The data represent the means \pm standard deviation (SD) ($n = 3$). Data of non-treated PET overlap with those of Sample 2.

3.3.2. X-Ray Photoelectron Spectroscopy (XPS) measurements

XPS measurements were performed using dry and hydrated polymer-coated PET substrates after freeze-drying in a water-contact environment. The results are listed in Table 5 and indicate that the theoretical F/C values of Samples 1–3 were lower than those of the experimental values. Containing the lowest *m*PEGMA amount, Sample 1 displayed the same values for both dry and hydrated conditions and was detected with the highest fluorine content. For dry Samples 2 and 3, the F/C ratio decreased when in contact with water, and more *m*PEGMA segregated at the interface with water. These results are in good agreement with the CA analyses.

Table 5. XPS data of the substrates coated with the investigated polymers before and after freeze-drying, dry and wet, respectively.

Polymers	Theoretical value	Dry				Wet			
	F _{1s} /C _{1s}	C _{1s}	O _{1s}	F _{1s}	F _{1s} /C _{1s}	C _{1s}	O _{1s}	F _{1s}	F _{1s} /C _{1s}
Sample 1	0.60	45.7	17.9	36.4	0.80	45.8	17.8	36.4	0.80
Sample 2	0.21	56.3	25.7	18.0	0.32	59.1	25.9	15.0	0.25
Sample 3	0.05	62.2	30.3	7.5	0.12	62.9	30.6	6.5	0.10
PFAHFiP	1.17	42.2	13.9	43.9	1.04	43.3	14.2	42.6	0.98
PMEA	0	68.7	31.3	0.0	0.0	68.5	31.6	0.0	0.00

3.4. Biocompatible properties: Protein adsorption and platelet adhesion of surfaces coated with the investigated polymer films

The amount of adsorbed fibrinogen and adhesion of platelets from human blood on the surface of homopolymers and copolymers, and on the reference surfaces of PMEA, PET, and polypropylene (PP) are presented in Figures 5 and 6. It is known that the degree of cell adhesion to PMEA and its analogous polymers' surface differs depending on the cell types, such as HT-1080, MDA-MB-231, HepG2 and human platelets.^{43,56} By comparing the adhesion behavior of human platelets which are one of the most investigated cells on PMEA, it is possible to estimate the extent of repelling properties of the new materials. The hydrophobic PET, PP, and fluorinated homopolymers displayed high amounts of adsorbed fibrinogen and adhered platelets on their surfaces. In contrast to the fluorinated homopolymers and PP substrate, on the surfaces of the synthesized copolymers (Samples 1–3) a lower adsorbed fibrinogen amount was found. A similar tendency was observed for platelet adhesion. Increasing the *m*PEGMA amount from

Samples 1 to 3 induced a decrease in both the amounts of adsorbed protein and adhered platelets. Samples 2 and 3 contained considerably lower amounts of both components compared to those of Sample 1. PMEA is known for its excellent bio-inert properties,^{3,45,47} which are improved in some of its homologues.^{43,44,46} Therefore, the present investigation clearly displays that the bio-inert properties of the synthesized copolymers 2 and 3 are superior to those of the PMEA homopolymer.

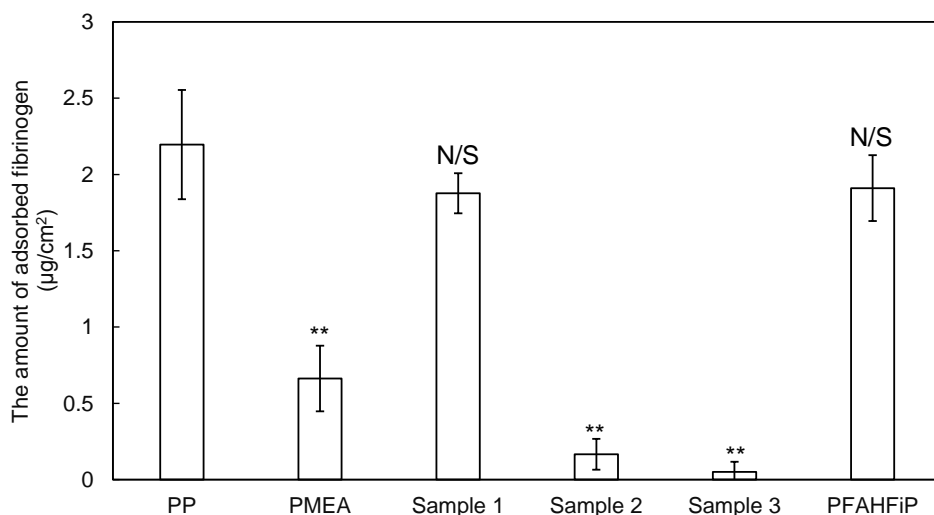


Figure 5. Amount of adsorbed fibrinogen determined by the micro-BCA method. The data represent the means \pm SD ($n = 3$) of fibrinogen adsorption. ** $p < 0.01$ vs. PP. N/S is an abbreviation for Not Significant.

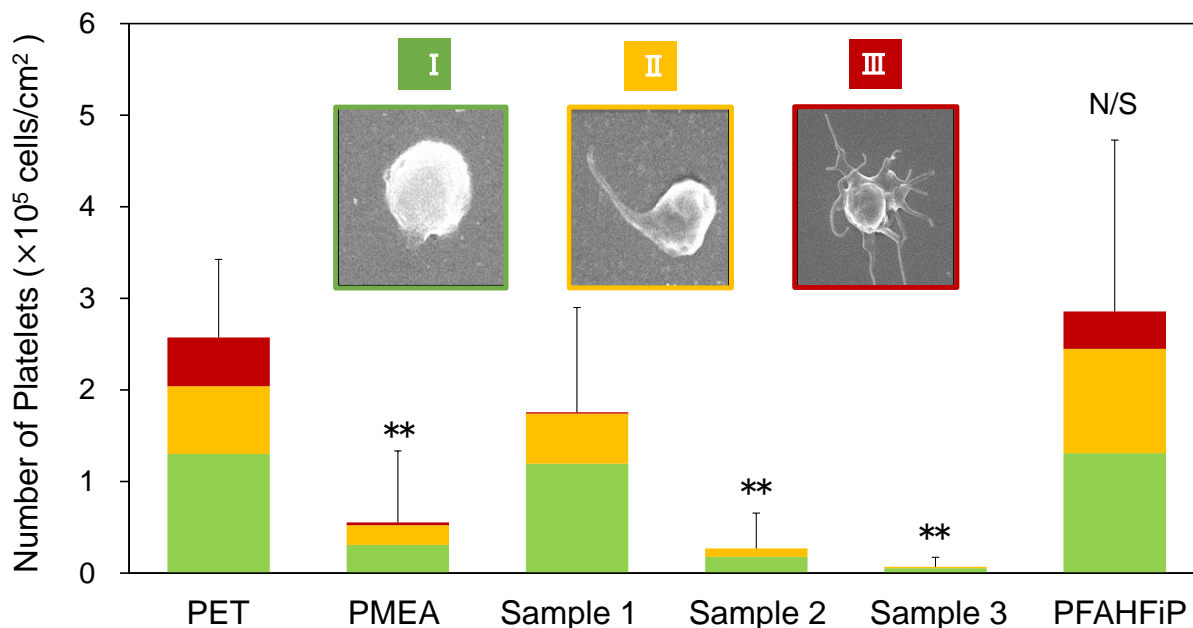


Figure 6. Number of adhered platelets on all the studied materials. Types I, II, and III signify different platelet morphologies. The data represent the means \pm SD ($n = 15$; 15 points \times 3 substrates). * $p < 0.05$, ** $p < 0.01$ vs. PET. N/S is an abbreviation for Not Significant.

According to the degree of activation, the adhered platelets (Figure 6) are classified into three types: type I are spherical-shaped native platelets, II are partially activated hemispherical platelets with several pseudopods, while III are activated platelets with a spread shape and numerous *pseudopods* or flat discoid. **Usually a very small amount of platelets adheres to PMEA and therefore this polymer prevents the activation of adhered platelets (Type III).** A similar tendency was observed for Sample 1, whereas Samples 2 and 3 displayed no type III platelets. The number of type II platelets decreased in the order of increasing *m*PEGMA content of the fluorinated copolymers. This indicates that a copolymer composed of a higher amount of the hydrophilic, water-soluble *m*PEGMA and a smaller PFAHFiP content exhibits improved bio-

inertness of the resulting material. Therefore, Sample 3 displays the best blood compatibility with the highest *m*PEGMA content while retaining its insolubility in water. The SEM pictures (Figure S9) visually show the adhered platelets on the fluorinated copolymer samples.

3.5. Relationship of the hydrated structures with biocompatibility

3.5.1. Atomic Force Microscopy (AFM)

The interface morphology of the fluorinated copolymer samples in the dry and hydrated states after immersion in water for 1 and 24 h was evaluated by AFM. Some morphological changes were observed; however, the detailed features of the interfaces were unclear (Figure S10). Therefore, we focused on the deformation of the film as measured by the peak force tapping mode of the Bruker BioScope Resolve AFM instrument and observed in water after 24 h-immersion.

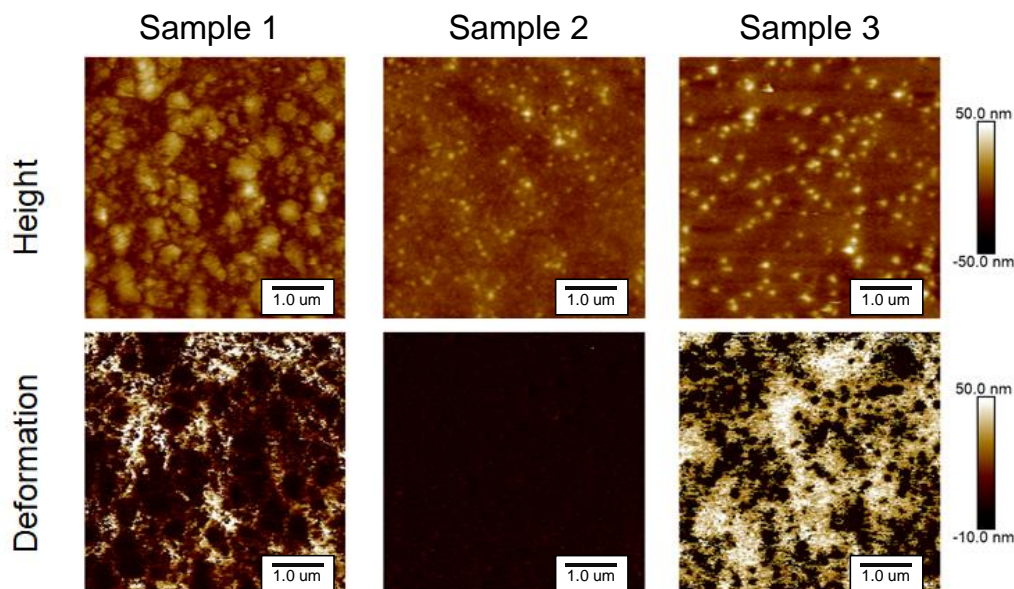


Figure 7. AFM images (height and deformation) of Samples 1–3. (The scale bar is 1.0 μm)

Samples 1 and 3 induced phase separation of the fluorinated polymer and *m*PEGMA (Figure 7). The dark areas in the deformation images display small deformations (rich in fluorinated polymer), whereas the bright areas display large deformations (*m*PEGMA-rich). Thus, Sample 1 had the largest fraction of fluorinated polymer domains, while Sample 3 had the lowest fraction, corresponding to the increase in *m*PEGMA content from Samples 1–3. Sample 2 was virtually homogeneous, which was consistent with the absence of any phase separation. This finding may be explained by the composition of the sample, as well as its broader dispersity (4.51) compared to those of the other samples (1.77–2.17) (Table 2). Higher dispersity (PDI) may have prevented from the apparent phase separation and led to a homogeneous structure.

From the AFM deformation data (Figure 7), the bright areas assigned to the *m*PEGMA domains were masked. The area percentages on the interface of the copolymer with water were calculated using NanoScope Analysis software (Bruker) (Figure S11).

Sample 1 contained 18.0% *m*PEGMA domains at the polymer–water interface. This means that most of the interface (82.0%) was occupied by the FAHFiP component. This content was more than tripled in Sample 3 (55.6%). The interface of Sample 2 was almost homogeneous, but the deformation value was low, approaching the value of the FAHFiP-rich domains. Therefore, the interface of Sample 2 was rich in the FAHFiP component. This finding was consistent with the bio-inert properties of the synthesized samples discussed above.

3.5.2. Bio-inert properties of the investigated materials

The significantly larger amount of hydrophilic moiety in Sample 3 at the interface with water as compared to that of Sample 1 (determined by AFM) correlates well with the decreased

amount of adsorbed proteins and number of adhered platelets. Moreover, the *m*PEGMA domains with large deformations, as displayed in Figure 7, prevent the adhesion of platelets at a higher degree (Figure 6). Therefore, the hydrated structures influenced the bio-inert properties of the materials.

Furthermore, the protein or platelet quantities detected on the surface displayed good correlation with IWC (Figure 8). In principle, higher amounts of *IW* detected in polymers indicated better bio-inert properties. Additionally, even with higher WCA and ACA values compared to those of the blood-compatible PMEA, the copolymers displayed higher hydrophilicity and superior bio-inert properties when in contact with water. Finally, enrichment of the polymer–water interface with an increased number of hydrophilic domains with larger deformation was visualized by AFM. This enrichment was due to morphological changes of the dry and hydrated samples and efficient phase separation. All these statements, evidenced by the current investigations, add new examples to the copolymers of MEA and HEMA^{2,39,40} that display improved blood compatibility and bio-inert characteristics, when the copolymers contained small amounts of fluorinated moieties.

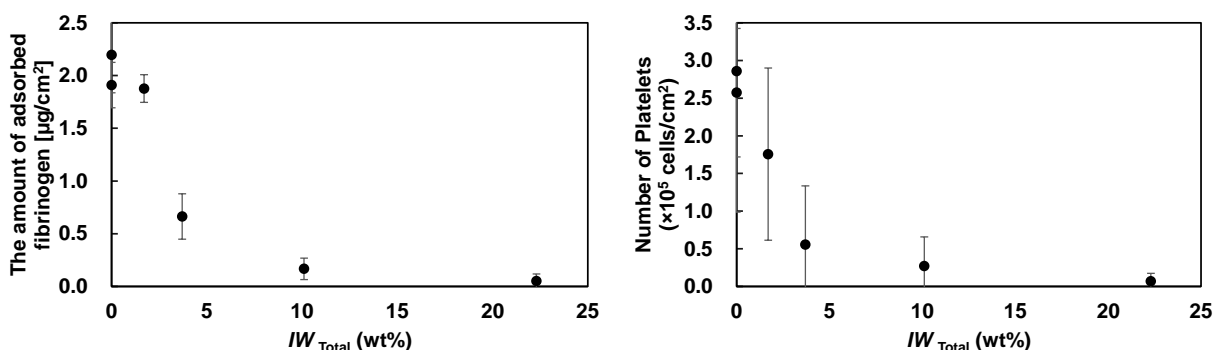


Figure 8. Relationship between the measured IWC and fibrinogen quantities (left) or platelets (right) on the surface of all investigated polymers

To comprehensively study the polymer–water interface, the differences in the analysis area sensitivity of each experiment should be considered. The properties of *m*PEGMA can be improved by copolymerization with a lower amount of FAHFiP. However, the adhesion behavior of fibrinogen or platelets of the same sample in the nanometer or micrometer order, respectively, was close to that of the homopolymer PFAHFiP. Considering the differences in the order of millimeters detected in the CA and XPS investigations, the results suggest that the microscopic area of the polymer–water interface of this copolymer was not sufficiently covered with hydrophilic sites and that the fluorinated sites were partially exposed (Figure 9). The copolymer with the lowest fluorinated monomer content of 15.2 mol % (7.9 wt%) remained insoluble in water because of the strong hydrophobicity of the fluorinated groups. The long *m*PEGMA chains stretched in water, and the sites containing *IW* covering a larger area of the interface (compared to the other copolymers with less *m*PEGMA) endowed the material with the best bio-inert properties, which were superior to those of PMEAs.

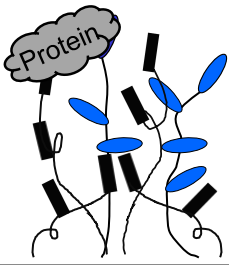
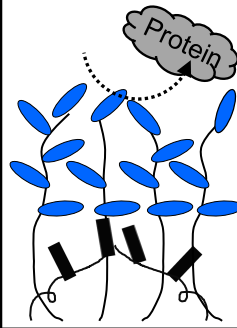
		Fluorine major	Fluorine minor
Hydration Structure			
Bulk		Water-insoluble	
Surface	Macroscopic area	Hydrophilic	
	Microscopic area	Partly hydrophobic	Hydrophilic

Figure 9. Conceptual image of hydration structure of poly(FAHFiP-*co*-*m*PEGMA) copolymers

4. Conclusions

Water-insoluble random copolymers based on the hydrophilic *m*PEGMA and a highly hydrophobic alpha-fluoroacrylate monomer, FAHFiP, were synthesized by conventional radical copolymerization. The hydration structures of these copolymers, the PMEA and PFAHFiP homopolymers, and the PP and PET substrates were evaluated using DSC, CA, XPS, AFM, platelet adhesion, and fibrinogen absorption and discussed. As displayed by ACA, the resulting poly(FAHFiP-*co*-*m*PEGMA) copolymer with the highest fluorine content (80.3 mol %) was hydrophilic at the macroscopic area of the polymer–water interface. The hydration structures displayed *IW*, which was related to the bio-inert properties of the material. AFM visualization exhibited that morphological changes and efficient phase separation enriched the polymer–water interface of the hydrated samples with hydrophilic domains. This study displayed that the addition of a small fluorine content to *m*PEGMA copolymers can efficiently segregate at the surface. Moreover, this work demonstrated that the presence of water improves the hydrophilicity of the polymer–water interface by exposing the hydrophilic *m*PEGMA to water and reducing the hydrophobicity of the surface. Compared to the blood-compatible PMEA, the random copolymers investigated in this work, which had low dry and hydrated T_g , exhibited increased hydrophilicity, IWC, WCA, and ACA, as well as improved bio-inert properties when in contact with water. These examples demonstrate that the addition of a small amount of the highly mobile, hydrophobic fluorine in hydrophilic materials alters the bulk and interface hydration states. Such results are expected to contribute to the development of improved bio-inert coatings for medical devices.

Associated Content

¹⁹F and ¹H NMR spectra, DSC thermograms, water contact angle images, SEM images of platelets adhered onto the surfaces and AFM images of poly(FAHFIP-*co*-mPEGMA) copolymers.

Author Information

Corresponding Author

*E-mail: masaru_tanaka@ms.ifoc.kyushu-u.ac.jp and bruno.ameduri@enscm.fr

ORCID

Ryohei Koguchi: 0000-0003-0017-4783

Katja Jankova: 0000-0002-4218-064X

Daiki Murakami: 0000-0002-5552-4384

Bruno Ameduri: 0000-0003-4217-6664

Masaru Tanaka: 0000-0002-1115-2080

Present Addresses

Daiki Murakami:

†Present affiliation: Department of Biological and Environmental Chemistry, Faculty of Humanity-Oriented Science and Engineering, Kindai University, 11-6 Kayanomori, Iizuka, Fukuoka, 820-8555, Japan

Acknowledgments

This work was supported by JSPS KAKENHI (Grant No. JP19H05720 and 22H00591), JST A-STEP and the AGC Research Collaboration System. This study was partially supported by the Dynamic Alliance for Open Innovation Bridging Human, Environment, and Materials. We acknowledge Project PROGRESS 100 from Kyushu University for its financial support. BA thanks the “French Fluorine Network” and the EU (grant agreement 647857-SENSOILS).

Notes

The authors declare no competing financial interest.

Abbreviations

Materials

PEG	Poly(ethylene glycol)
PEGMA	Poly(ethylene glycol) methacrylate
<i>m</i> PEGMA	Poly(ethylene glycol) methyl ether methacrylate
PMEA	Poly(2-methoxyethyl acrylate)

HEMA	2-Hydroxyethyl methacrylate
PHEMA	Poly(2-hydroxyethyl methacrylate)
TFEMA	2,2,2-Trifluoroethyl methacrylate
DMAEMA	2-(Dimethylamino)ethyl methacrylate
PFAHFIP	Poly(1,1,1,3,3,3-hexafluoropropan-2-yl) 2-fluoroacrylate
PP	Polypropylene
PET	Polyethylene terephthalate

Analyses

DSC	Differential Scanning Calorimetry
AFM	Atomic Force Microscope
XPS	X-ray Photoelectron Spectroscopy
NMR	Nuclear Magnetic Resonance
SEC	Size-Exclusion Chromatography
CA	Contact Angle
WCA	Water-in-air Contact Angle
ACA	Air-in-water Contact Angle

SEM Scanning Electron Microscopy

Interactions between Water and Polymers

NFW Non-freezing water

IW Intermediate water

FW Free water

WC Water content

NFWC Non-freezing water content

IWC Intermediate water content

FWC Free water content

EWC Equilibrium water content

References

1. Ratner, B. D.; Bryant, S. J. Biomaterials: where we have been and where we are going. *Annu. Rev. Biomed. Eng.* **2004**, *6*, 41-75.
2. Koguchi, R.; Jankova, K.; Tanaka, M. Fluorine-containing bio-inert polymers: Roles of intermediate water. *Acta Biomater* **2022**, *138*, 34-56.
3. Tanaka, M.; Motomura, T.; Kawada, M.; Anzai, T.; Kasori, Y.; Shiroya, T.; Shimura, K.; Onishi, M.; Mochizuki, A. Blood compatible aspects of poly (2-methoxyethylacrylate)(PMEA)—relationship between protein adsorption and platelet adhesion on PMEA surface. *Biomaterials* **2000**, *21*, 1471-1481.
4. Anzai, T.; Okumura, A.; Kawaura, M.; Yokoyama, K.; Oshiyama, H.; Kido, T.; Nojiri, C. Evaluation of the Biocompatibility of an In Vitro Test Using a Poly(2-methoxyethylacrylate) Coated Oxygenator. *Jpn. J. Artif. Organs* **2000**, *9*, 73-77.
5. Hoshiba, T.; Otaki, T.; Nemoto, E.; Maruyama, H.; Tanaka, M. Blood-compatible polymer for hepatocyte culture with high hepatocyte-specific functions toward bioartificial liver development. *ACS Appl. Mater. Interfaces* **2015**, *7*, 18096-18103.
6. Lee, W.; Kobayashi, S.; Nagase, M.; Jimbo, Y.; Saito, I.; Inoe, Y.; Yambe, T.; Sekino, M.; Malliaras, G. G.; Yokota, T.; Tanaka, M.; Someya, T. Nontrombogenic, stretchable, active multielectrode array for electroanatomical mapping. *Sci. Adv.* **2018**, *4*, No. eaau2426
7. Harris, J. M., Ed. *Poly(ethyleneglycol) chemistry: biotechnical and biomedical applications*; Plenum Press: New York, **1992**.
8. Yeh, C.-C.; Venault, A.; Chang, Y. Structural Effect of Poly(Ethylene Glycol) Segmental Length on Biofouling and Hemocompatibility. *Polym. J.* **2016**, *48*, 551-558.
9. Holmlin, R. E.; Chen, X.; Chapman, R. G.; Takayama, S.; Whitesides, G. M. Zwitterionic SAMs that resist nonspecific adsorption of protein from aqueous buffer. *Langmuir* **2001**, *17*, 2841-2850.
10. Thom, V.; Jankova, K.; Ulbricht, M.; Kops, J.; Jonsson, G. Synthesis of photoreactive α -4-azidobenzoyl- ω -methoxy-poly(ethylene glycol)s and their end-on photo-grafting onto polysulfone ultrafiltration membranes. *Macromol. Chem. Phys.* **1998**, *199*, 2723-2729.
11. Thom, V. H.; Altankov, G.; Groth, T.; Jankova, K.; Jonsson, G.; Ulbricht, M. Optimizing cell-surface interactions by photografting of poly(ethylene glycol). *Langmuir* **2000**, *16*, 2756-2765.

12. Altankov, G.; Thom, V.; Groth, T.; Jankova, K.; Jonsson, G.; Ulbricht, M. Modulating the biocompatibility of polymer surfaces with poly (ethylene glycol): effect of fibronectin. *J. Biomed. Mater. Res.* **2000**, *52*, 219-230.
13. Røn, T.; Javakhishvili, I.; Patil, N. J.; Jankova, K.; Zappone, B.; Hvilsted, S.; Lee, S. Aqueous lubricating properties of charged (ABC) and neutral (ABA) triblock copolymer chains. *Polymer* **2014**, *55*, 4873-4883.
14. Han, D. K.; Park, K. D.; Ryu, G. H.; Kim, U. Y.; Min, B. G.; Kim, Y. H. Plasma protein adsorption to sulfonated poly (ethylene oxide)- grafted polyurethane surface. *Journal of Biomedical Materials Research: An Official Journal of The Society for Biomaterials and The Japanese Society for Biomaterials* **1996**, *30*, 23-30.
15. Barbey, R.; Lavanant, L.; Paripovic, D.; Schuwer, N.; Sugnaux, C.; Tugulu, S.; Klok, H. Polymer brushes via surface-initiated controlled radical polymerization: synthesis, characterization, properties, and applications. *Chem. Rev.* **2009**, *109*, 5437-5527.
16. Xu, F. J.; Neoh, K. G.; Kang, E. T. Bioactive surfaces and biomaterials via atom transfer radical polymerization. *Prog. Polym. Sci.* **2009**, *34*, 719-761.
17. Fristrup, C. J.; Jankova, K.; Hvilsted, S. Surface-initiated atom transfer radical polymerization—A technique to develop biofunctional coatings. *Soft Matter* **2009**, *5*, 4623-4634.
18. Fristrup, C. J.; Jankova, K.; Hvilsted, S. Hydrophilization of poly (ether ketone) films by surface-initiated atom transfer radical polymerization. *Polym. Chem.* **2010**, *1*, 1696-1701.
19. Fristrup, C. J.; Jankova, K.; Eskimerger, R.; Bukrinsky, J. T.; Hvilsted, S. Protein repellent hydrophilic grafts prepared by surface-initiated atom transfer radical polymerization from polypropylene. *Polym. Chem.* **2012**, *3*, 198-203.
20. Fristrup, C. J.; Jankova, K.; Eskimerger, R.; Bukrinsky, J. T.; Hvilsted, S. Stability of AspB28 Insulin Exposed to Modified and Unmodified Polypropylene. *Protein Pept. Lett.* **2015**, *22*, 1-9.
21. Ishihara, K.; Ueda, T.; Nakabayashi, N. Preparation of phospholipid polymers and their properties as polymer hydrogel membranes. *Polym. J.* **1990**, *22*, 355-360.
22. Jeon, S. I.; Lee, J. H.; Andrade, J. D.; De Gennes, P. Protein—surface interactions in the presence of polyethylene oxide: I. Simplified theory. *J. Colloid Interface Sci.* **1991**, *142*, 149-158.
23. Jankova, K.; Chen, X.; Kops, J.; Batsberg, W. Synthesis of amphiphilic PS-b-PEG-b-PS by atom transfer radical polymerization. *Macromolecules* **1998**, *31*, 538-541.

24. McPherson, T.; Kidane, A.; Szleifer, I.; Park, K. Prevention of protein adsorption by tethered poly (ethylene oxide) layers: experiments and single-chain mean-field analysis. *Langmuir* **1998**, *14*, 176-186.
25. Ishihara, K. Bioinspired phospholipid polymer biomaterials for making high performance artificial organs. *Sci. Technol. Adv. Mater.* **2000**, *1*, 131.
26. Jankova, K.; Jannasch, P.; Hvilsted, S. Ion conducting solid polymer electrolytes based on polypentafluorostyrene-b-polyether-b-polypentafluorostyrene prepared by atom transfer radical polymerization. *J. Mater. Chem.* **2004**, *14*, 2902-2908.
27. Uchida, K.; Hoshino, Y.; Tamura, A.; Yoshimoto, K.; Kojima, S.; Yamashita, K.; Yamanaka, I.; Otsuka, H.; Kataoka, K.; Nagasaki, Y. Creation of a mixed poly (ethylene glycol) tethered-chain surface for preventing the nonspecific adsorption of proteins and peptides. *Biointerphases* **2007**, *2*, 126-130.
28. Kyomoto, M.; Moro, T.; Yamane, S.; Hashimoto, M.; Takatori, Y.; Ishihara, K. Poly (ether-ether-ketone) orthopedic bearing surface modified by self-initiated surface grafting of poly (2-methacryloyloxyethyl phosphorylcholine). *Biomaterials* **2013**, *34*, 7829-7839.
29. Hoang Thi, T. T.; Pilkington, E. H.; Nguyen, D. H.; Lee, J. S.; Park, K. D.; Truong, N. P. The importance of poly (ethylene glycol) alternatives for overcoming PEG immunogenicity in drug delivery and bioconjugation. *Polymers* **2020**, *12*, 298.
30. Hansen, N. M.; Jankova, K.; Hvilsted, S. Fluoropolymer materials and architectures prepared by controlled radical polymerizations. *Eur. Polym. J.* **2007**, *43*, 255-293.
31. Smith, D. W.; Iacono, S. T.; Iyer, S. S. *Handbook of fluoropolymer science and technology*; John Wiley & Sons: **2014**. p. 672
32. Honda, K.; Yamamoto, I.; Morita, M.; Yamaguchi, H.; Arita, H.; Ishige, R.; Higaki, Y.; Takahara, A. Effect of α -substituents on molecular motion and wetting behaviors of poly (fluoroalkyl acrylate) thin films with short fluoroalkyl side chains. *Polymer* **2014**, *55*, 6303-6308.
33. Aandei, A. D. Photomediated Controlled Radical Polymerization and Block Copolymerization of Vinylidene Fluoride. *Chem. Rev.* **2016**, *116* (4), 2244–2274.
34. Zapsas, G.; Patil, Y.; Gnanou, Y.; Ameduri, B.; Hadjichristidis, N. Poly (vinylidene fluoride)-based complex macromolecular architectures: From synthesis to properties and applications. *Prog. Polym. Sci.* **2020**, *104*, 101231.
35. Ameduri, B. The promising future of fluoropolymers. *Macromol. Chem. Phys.* **2020**, *221*, 1900573.

36. Ameduri, B.; Fomin, S. *Fascinating Fluoropolymers and Their Applications*; Elsevier: Oxford, **2020**.
37. Ameduri, B.; Fomin, S. *Opportunities for Fluoropolymers: Synthesis, Characterization, Processing, Simulation and Recycling*; Elsevier: Oxford, **2020**.
38. Guerre, M.; Lopez, G.; Améduri, B.; Semsarilar, M.; Ladmiral, V. Solution self-assembly of fluorinated polymers, an overview. *Polym. Chem.* **2021**, *12*, 3852-3877.
39. Koguchi, R.; Jankova, K.; Tanabe, N.; Amino, Y.; Hayasaka, Y.; Kobayashi, D.; Miyajima, T.; Yamamoto, K.; Tanaka, M. Controlling the hydration structure with a small amount of fluorine To produce blood compatible fluorinated poly (2-methoxyethyl acrylate). *Biomacromolecules* **2019**, *20*, 2265-2275.
40. Koguchi, R.; Jankova, K.; Hayasaka, Y.; Kobayashi, D.; Amino, Y.; Miyajima, T.; Kobayashi, S.; Murakami, D.; Yamamoto, K.; Tanaka, M. Understanding the effect of hydration on the bio-inert properties of 2-hydroxyethyl methacrylate copolymers with small amounts of amino-or/and fluorine-containing monomers. *ACS Biomater. Sci. Eng.* **2020**, *6*, 2855-2866.
41. Takahashi, S.; Kasemura, T.; Asano, K. Surface molecular mobility for copolymers having perfluorooctyl and/or polyether side chains via dynamic contact angle. *Polymer* **1997**, *38*, 2107-2111.
42. Zhao, Z.; Ni, H.; Han, Z.; Jiang, T.; Xu, Y.; Lu, X.; Ye, P. Effect of surface compositional heterogeneities and microphase segregation of fluorinated amphiphilic copolymers on antifouling performance. *ACS Appl. Mater. Interfaces* **2013**, *5*, 7808-7818.
43. Sato, K.; Kobayashi, S.; Kusakari, M.; Watahiki, S.; Oikawa, M.; Hoshihara, T.; Tanaka, M. The Relationship Between Water Structure and Blood Compatibility in Poly(2-methoxyethyl Acrylate) (PMEA) Analogues. *Macromol. Biosci.* **2015**, *15* (9), 1296–1303.
44. Kobayashi, S.; Wakui, M.; Iwata, Y.; Tanaka, M. Poly (ω -methoxyalkyl acrylate) s: Nonthrombogenic polymer family with tunable protein adsorption. *Biomacromolecules* **2017**, *18*, 4214-4223.
45. Tanaka, M.; Kobayashi, S.; Murakami, D.; Aratsu, F.; Kashiwazaki, A.; Hoshihara, T.; Fukushima, K. Design of Polymeric Biomaterials: The “Intermediate Water Concept”. *Bull. Chem. Soc. Jpn.* **2019**, *92* (12), 2043-2057.
46. Sonoda, T.; Kobayashi, S.; Herai, K.; Tanaka, M. Side-chain spacing control of derivatives of poly (2-methoxyethyl acrylate): impact on hydration states and antithrombogenicity. *Macromolecules* **2020**, *53*, 8570-8580.
47. Tanaka, M.; Morita, S.; Hayashi, T. Role of interfacial water in determining the interactions of proteins and cells with hydrated materials. *Colloids Surf., B* **2021**, *198*, 111449.

48. Banerjee, S.; Tawade, B. V.; Ladmiral, V.; Dupuy, L. X.; MacDonald, M. P.; Améduri, B. Poly (fluoroacrylate) s with tunable surface hydrophobicity via radical copolymerization of 2, 2, 2-trifluoroethyl α -fluoroacrylate and 2-(trifluoromethyl) acrylic acid. *Polym. Chem.* **2017**, *8*, 1978-1988.
49. Hu, P.; Jiang, T.; Ni, H.; Ye, P.; Han, Z.; Zhao, Z.; Zhu, C.; Lu, X. Synthesis, characterization and antifouling performance of ABC-type fluorinated amphiphilic triblock copolymer. *Polym. Bull.* **2016**, *73*, 1405-1426.
50. Li, Y.; Qian, W.; Huang, J.; Zhou, X.; Zuo, B.; Wang, X.; Zhang, W. Critical domain sizes of heterogeneous nanopattern surfaces with optimal protein resistance. *J. Phys. Chem. C* **2018**, *122*, 9918-9928.
51. Pittman, C. U.; Ueda, M.; Iri, K.; Imai, Y. Synthesis and Polymerization of Methyl α -Fluoroacrylate. *Macromolecules*, **1980**, *13*(5), 1031-1036.
52. Cracowski, J. M.; Montebault, V.; Améduri, B. Free- radical copolymerization of 2, 2, 2- trifluoroethyl methacrylate and 2, 2, 2- trichloroethyl α - fluoroacrylate: Synthesis, kinetics of copolymerization, and characterization. *J. Polym. Sci., Part A: Polym. Chem.*, **2010**, *48*(10), 2154-2161.
53. Golzari, N.; Adams, J.; Beuermann, S. Inducing β Phase Crystallinity in Block Copolymers of Vinylidene Fluoride with Methyl Methacrylate or Styrene. *Polymers* **2017**, *9*, 306-322.
54. Banerjee, S.; Patil, Y.; Gimello, O.; Ameduri, B. Well-defined multiblock poly(vinylidene fluoride) and block copolymers thereof: a missing piece of the architecture puzzle. *Chem. Commun.* **2017**, *53*, 10910–10913
55. Iborra, A.; Salvatierra, L.; Giussi, J. M.; Azzaroni, O. Synthesis of lauryl methacrylate and poly (ethylene glycol) methyl ether methacrylate copolymers with tunable microstructure and emulsifying properties. *Eur. Polym. J.* **2019**, *116*, 117-125.
56. Hoshiba, T.; Nemoto, E.; Sato, K.; Orui, T.; Otaki, T.; Yoshihiro, A.; Tanaka, M. Regulation of the Contribution of Integrin to Cell Attachment on Poly(2-Methoxyethyl Acrylate) (PMEA) Analogous Polymers for Attachment-Based Cell Enrichment. *PLoS One* **2015**, *10*, No. e0136066.

For table of Comments use only

Table of Contents Graphic.

